

Study of Wear Stabilisation in Cryoprocessed Cobalt-Based High Speed Steel

N. B. Dhokey · J. V. Dandawate

Received: 16 November 2011 / Accepted: 22 May 2012 / Published online: 17 June 2012
© Indian Institute of Metals 2012

Abstract Cryogenic treatment is employed for high speed tool steels in order to enhance their wear resistance. The improvement in wear resistance is associated with a decrease in retained austenite and or by formation of eta-carbide/nano-scale carbides. In the present work, a complex alloyed high speed tool steel (M35) specimens were hardened at 1,200 °C, triple tempered at 400 °C, cryosoaked at –185 °C for 4–48 h and soft tempered (100 °C). The microstructure of the samples were characterised for hardness, carbide density, impact energy, wear loss and residual stress. Influence of these measured parameters on wear behaviour was studied to understand underlying wear mechanism. The cryotreated specimens exhibited mild to stable wear transition at 16 h and then subsequent wear stabilisation for all higher cryosoaking intervals.

Keywords M35 steel · Residual stress · Wear stabilisation · Wear mechanism

1 Introduction

Most studies on cryogenic treatment are focused on M2 tool steel and little has been reported on cryogenic treatment of M35 tool steel containing cobalt, which is a modified grade of M2 tool steel. M35 is expected to impart better service life than M2 tool steel. da Silva et al. [1] have reported reduction of retained austenite very close to 0 % in M2 steel originally containing 25 vol% of retained austenite after cryogenic treatment. Molinari et al. [2] vacuum quenched M2 steel after

hardening at 1,220 °C, double tempered at 540 °C and cryotreated at –196 °C for 35 h. The lowest wear rate was observed when cryotreatment was introduced in between quenching and tempering. Barron [3] subjected 19 steels which included 12 types of tool steels, three types of stainless steels and four other types of steels to cryogenic treatments to determine the effect of –84 °C (189 K) soak and –196 °C (77 K) soak on the abrasive wear resistance. The results indicated that for the steels, the wear resistance was significantly improved by subjecting the samples to a long soak (>20 h) at 77 K. Huang et al. [4] soaked some samples of M2 in liquid nitrogen continuously for 1 week. Subsequently both the cryogenic treated and non-cryogenic treated samples were tempered at 200 °C in nitrogen atmosphere for 24 h. The cryogenic treatment not only facilitated the carbide formation and increase in the carbide population (volume fraction) in martensite matrix but also made the carbide distribution more homogeneous. The increase in carbide density and their volume fraction was responsible a notable improvement in wear resistance. Yong et al. [5] showed that cryogenic treatment improved the resistance to chipping of tools and thus improved the flank wear resistance of tungsten carbide tool inserts. Cryogenically treated tools perform better than untreated tools while performing continuous cutting for shorter periods of time. Alexandru et al. [6] quantified the precipitated carbides in M2 steel and verified their influence onto the material properties. Their research involved seven steel samples with each one of them subjected to different heating and cooling (up to –70 °C) cycles. The results confirmed an increase in carbide precipitation (from 6.9 to 17.4 %), a reduction of the retained austenite (from 42.6 to 0.9 %) and an increase in the martensite content (from 66 to 81.7 %). Subsequent machining carried out by turning AISI 1050 steels showed a significant increase in tool life of cryogenically treated tools. Meng et al. [7] carried out

N. B. Dhokey (✉) · J. V. Dandawate
Department of Metallurgical Engineering, Government College
of Engineering, Pune 411005, India
e-mail: nbdhokey@yahoo.co.in

cryotreatment on 12CrMoV1.4C type tool steel and reported improvement in the wear resistance as a result of precipitation of η -carbides in the martensitic matrix, revealed in high resolution TEM study. The size of η -carbides was in the range of 5–10 nm. Yang et al. [8] gave cryogenic treatment to tool steel (2.78 %C, 12.70 %Cr, 1.6 %V) at $-196\text{ }^{\circ}\text{C}$ for 3 h, followed by warming up to $1,000\text{ }^{\circ}\text{C}$ and then air cooling. The cryotreated steel gave homogeneous distribution of secondary carbides as compared to cast tool steel. Leskovsek and Kalin [9] treated one set of M2 samples for single and double cycle of varying tempering temperatures ($500\text{--}660\text{ }^{\circ}\text{C}$) and another set of samples by cryogenic treatment at $-196\text{ }^{\circ}\text{C}$ for 1 h followed by single tempering. Firouzdor et al. [10] reported improvement in wear resistance for M2 tool drill to the tune of 77 % in hardened and simply cryotreated ($-185\text{ }^{\circ}\text{C}$ for 24 h) condition without any post tempering and 126 % in hardened, cryotreated and post tempering condition. Kelkar et al. [11] studied fundamental aspect of M2 tool steel by subjecting to various combination of hardening, cryotreatment ($-195\text{ }^{\circ}\text{C}$ for 40 h) and triple tempering (TTT, $565\text{ }^{\circ}\text{C}$). It is observed that cryotreatment followed by single tempering eliminated residual strain to the maximum level. Khan and Ahmed [12] studied machining performance of SUS 304 steel using coated carbide inserts. In order to avoid heat generation due to plastic deformation, direct liquid nitrogen was employed in the cutting shear zone. The tool life increased four times due to use of liquid nitrogen as a coolant. Das et al. [13] investigated influence of varying holding time at cryogenic treatment temperature ($185\text{ }^{\circ}\text{C}$) on AISI D-2 steel, wherein cryotreatment was introduced in between quenching and tempering. The holding time of 24–36 h yielded optimum wear performance.

From the above cited literature available to the authors, it is clearly revealed that there is inadequate knowledge on cryoprocessing of M35 tool steel particularly in exploring wear mechanism and wear stability over a period of cryosoaking time.

2 Experimental Methods and Materials

2.1 Selection of Material

The M35 tool steel was in the form of rod of 10 mm diameter. Vacuum emission spectrometer was used for chemical analysis indicated composition as 0.9C, 6.0W, 5.2Mo, 4.0Cr, 1.7V, 4.7Co (by wt%).

2.2 Hardening and Tempering

Hardening of M35 tool steel was done in a sintering tubular furnace (Therlek, 3.8 KW, 230 V, AC, $1,600\text{ }^{\circ}\text{C}$) by controlled heating in stages of $550\text{ }^{\circ}\text{C}$, then $900\text{ }^{\circ}\text{C}$ for half an

hour under argon atmosphere, and finally $1,200\text{ }^{\circ}\text{C}$ for 2 min followed by quenching in oil stirred bath. After hardening, the TTT was carried out at $400\text{ }^{\circ}\text{C}$ for 2 h for each tempering cycle, followed by air cooling to room temperature. The specimen treated in this manner was designated as heat treated specimens (HTTT).

2.3 Post Cryogenic Treatment

The post cryogenic treatment, as shown in Fig. 1, was given in a computer controlled cryoprocessor (make: Sandmar, Mumbai, minus $185\text{ }^{\circ}\text{C}$) to conventionally HTTT as described in Sect. 2.2. Tool steel specimens were put in cryoprocessor at room temperature before starting the cycle and then the temperature of the processor was brought down at a cooling rate of $3\text{ }^{\circ}\text{C}/\text{min}$ by supplying calculated gasified liquid nitrogen through solenoid valve. The cryosoaking time was varied from 4 to 48 h. After regular interval of cryosoaking time, the specimens were removed from the cryoprocessor and immediately transferred and stored in a highly insulated thermocol box till the specimens attain the room temperature. A specimen processed in this manner, for example, for 4 h cryosoaking time, is designated as HTC4.

2.4 Characterization

Rockwell hardness tester was used for measurement of hardness on C-scale. The flat surface was prepared by using 1/0 paper. A minor load of 10 kg was first applied to seat the indenter. Then major load of 150 kg was applied for 15 s and resistance to indentation was recorded on the dial gauge. An average of five readings was noted as a measure of hardness. Charpy impact specimen was used to measure the impact energy (Joules) by digital impact test machine (make: FIE, least count 0.5 J). Freshly prepared charpy impact test specimens treated as per procedure described in

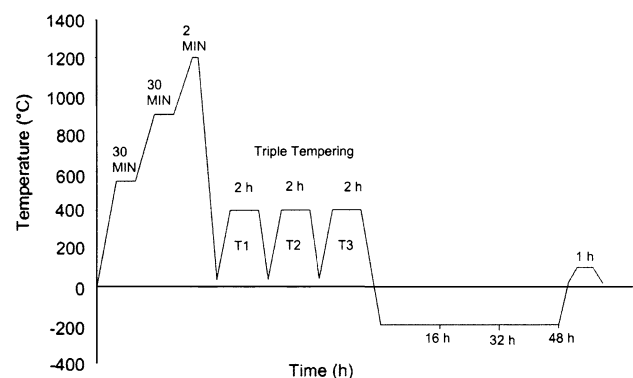


Fig. 1 Schematic T-T diagram illustrates processing steps employed on M35 tool steel

Sects. 2.2 and 2.3 were tested for impact toughness. An average for three readings was taken as a measure of impact energy. Pin-on-disc test machine (make: Magnum Engineer, Bangalore) was used for dry sliding wear in which stationary pin made out of M35 tool steel was slid against counterface disc. Pin of 10 mm diameter and 15 mm height was slid on the circular rotating disc of SAE52100 for a sliding distance of 6,000 m at an applied pressure of 60 N and 2.5 m/s sliding speed. The diameter of counterface disc was 170 mm with hardness of 59 HRC.

A usual metallographic polishing technique was followed in sequential manner on emery paper (1/0, 2/0, 3/0 and 4/0) so as to make surface free from scratches. Final polishing was done on velvet cloth lapped polishing machine with intermittent application of fine suspensions of alumina to get better finish on polished surface. A freshly prepared etchant 3 % nital was used for revealing microconstituents. Etched samples were observed in inverted metallurgical microscope (make: Carl Zeiss) and scanning electron microscope (make: JOEL). Microstructures of SEM at fixed magnification of 2,000 \times for all cryosoaking time were used for manual counting of carbides. In this, coarse carbide (CC) of diameter more than 1 μm and fine carbide (FC) less than and equal to 1 μm were separately counted and expressed as number of carbides per unit area as carbide density.

Specimens of 3 mm thickness and 10 mm diameter were cut into thin slices of 3 mm thick and 12 mm diameter using diamond saw machine. Residual stress was carried using copper target in XRD (Make: X'Pert PRO PAN analytical, Goniometer-PW3050/65, specimen Stage-MRD i.e. material research diffraction cradle) machine at Indian Institute of Technology Bombay.

3 Results and Discussion

3.1 Microstructural Features

Some representative microstructures are shown in Fig. 2 to depict carbide distribution pattern. Microstructure of HTTT specimens essentially consists of primary carbides and secondary carbides as evident in Fig. 2a. Further, cryosoaking can influence precipitation of tertiary carbides in the tempered martensitic structure as evident in Fig. 2b, c. Meng et al. [7] reported that cryogenic treatment facilitates the nano-scale carbide precipitation. Besides nucleation of tertiary carbides, the possibility of coarsening of carbides cannot be ruled out with increasing cryosoaking time. Carbide density variation with varying time is indicated in Fig. 3. It may be noted that maximum carbide density is observed at 16 h of cryosoaked time and thereafter fall in carbide density is seen which might be the result of

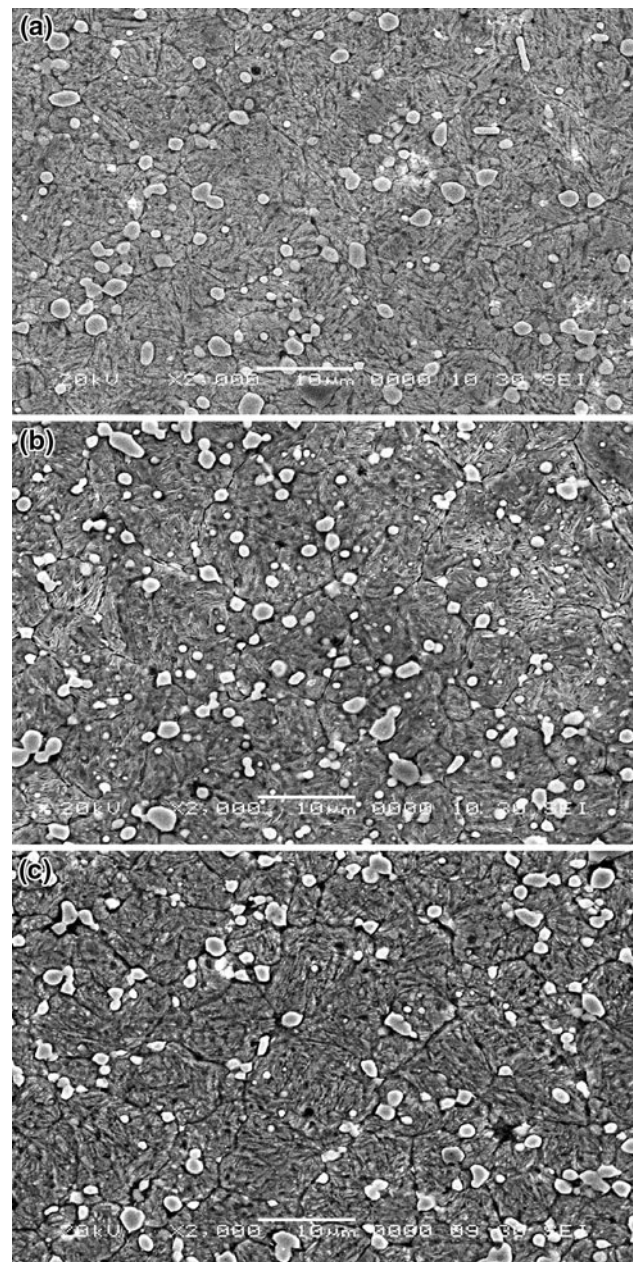


Fig. 2 SEM microstructures showing distribution of FC and CC in tempered martensitic matrix **a** HTTT, **b** HTC16 and **c** HTC48

coarsening of carbide by following Oswald ripening mechanism as explained by Reed-Hill [14]. The overall FCs are more than that of CCs in all cryotreated samples. Carbide density for FC is relatively more, suggesting high driving force for carbide precipitation of certain type of carbides.

3.2 Hardness Variation

Figure 4 indicates variation of hardness affected by cryosoaking time which depicts analogous pattern to the

carbide density variation (Fig. 3). The peak hardness is seen at 16 h which might be the results of high rate of nucleation of tertiary carbides compared to the rate of carbide growth. Beyond 16 h of cryosoaking time, there is drastic drop in hardness till 32 h of cryosoaking time which may be caused by coarsening of earlier formed carbides. A slight increase in hardness is noticed after 40 h of cryosoaking time. The highs and lows in the hardness variation graph can be attributed to rate of nucleation of tertiary carbides and coarsening of pre-existing carbides.

3.3 Impact Energy

It is observed from Fig. 5 that the overall trend shows gradual drop in impact energy with increase in cryosoaking time. It is least affected till 16 h of cryosoaking time, its value is almost close to the conventionally hardened and triple tempered steel. However, the value drops thereafter at 40 h which could be dominated by coarsening of carbides (Fig. 3) as well as drop in hardness (Fig. 4). After 40 h, however, impact energy increases till 48 h implies considerable rise in carbide density and hardness as well.

3.4 Residual Stress Analysis

Figure 6 shows that compressive stress gradually drops and attains minimum compressive stress at 16 h. Beyond 16 h, the compressive stress goes up and reaches a maxima at 24 h. It may be noted that residual stresses in matrix is normally originated in two ways (a) when specimen undergoes thermal processing wherein specimen experiences thermal shocks and (b) by the phase transformation particularly due to formation of martensite which manifests in the form of expansion of matrix. It is noticeable that minimum compressive stresses are seen at 16 h as a result

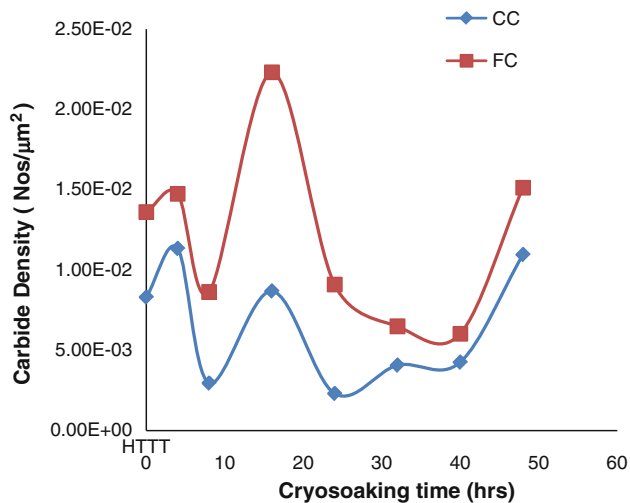


Fig. 3 Carbide density varying with cryosoaking time

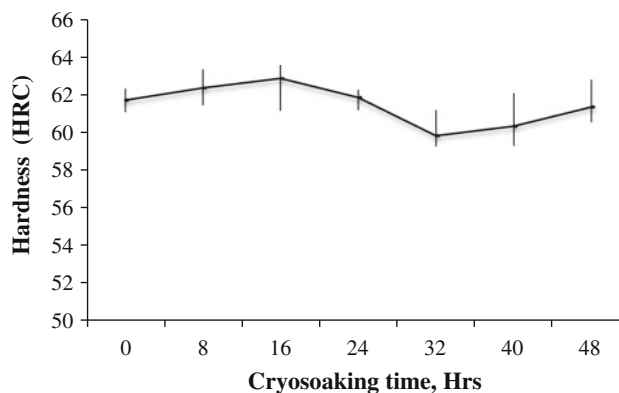


Fig. 4 Hardness variation as a function of cryosoaking time

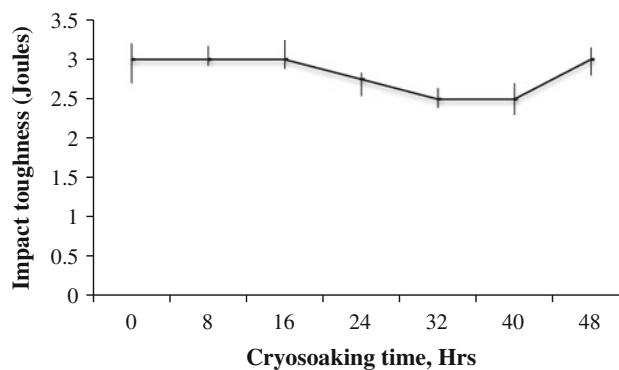


Fig. 5 Impact toughness varying with cryosoaking time

of more rate of nucleation of tertiary carbides in tempered martensitic matrix as noted from the carbide variation observed (Fig. 3) and the increase in hardness (Fig. 4). Thus nucleation relieves the matrix from stresses by way of precipitation of tertiary carbides in the tempered martensite. In the later part of cryosoaking period, greater than 24 h, the steel shows an increase in compressive residual stress that might be due to cryogenic treatment only.

3.5 Wear Behaviour

The wear rate variation may be correlated to hardness, impact energy, residual stress and carbide density as shown in Figs. 7, 8, 9 and 10. It is observed from analysis of wear behavior that variation in R² values signifies varying level of contribution of different factors. Thus wear rate is a complex phenomenon and affected by a number of influencing parameters. The wear rate provides partial correlation with other influencing parameters [15].

3.6 Wear Mechanism

The wear rate of cryotreated specimens is plotted as a function of cryosoaking time as shown in Fig. 11. With respect to HTTT, it is seen that there is dramatic drop in

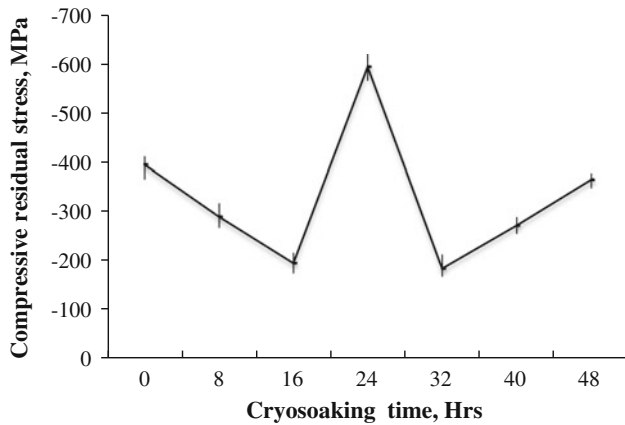


Fig. 6 Effect of cryosoaking time on residual stress

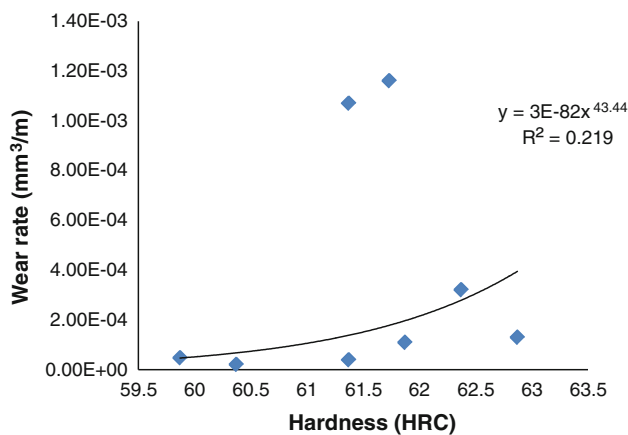


Fig. 7 Effect of hardness on wear rate of cryotreated tool steel

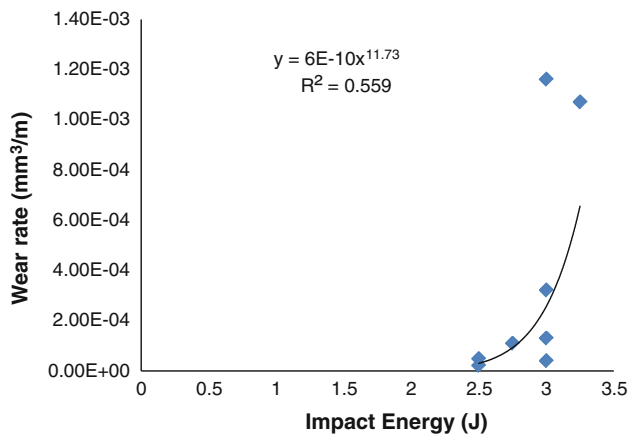


Fig. 8 Effect of impact energy on wear rate of cryotreated tool steel wear rate observed at 16 h of cryosoaking time, which amounts to reduction in wear rate by 90 %. Beyond this point, further drop in wear rate attains the level of saturation till 48 h of cryosoaking time which is analogous to wear stabilization. Thus the wear rate curve is divided into two parts depicting mild wear and stable wear regimes with well defined wear transition point.

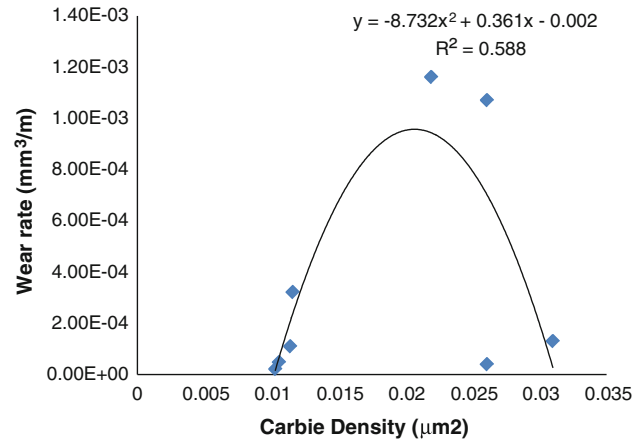


Fig. 9 Effect of carbide density (fine plus coarse) on wear rate of cryotreated tool steel

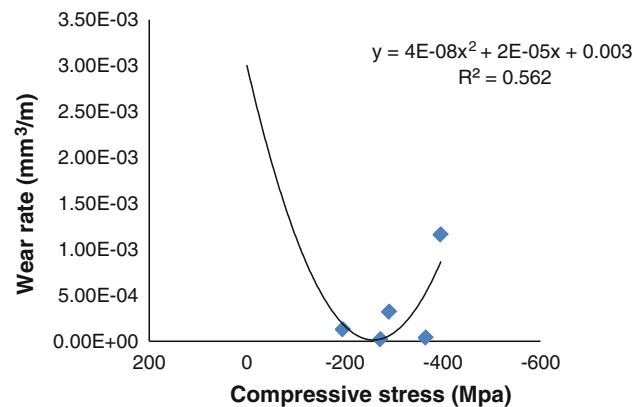


Fig. 10 Effect of compressive stress (residual stress) on wear rate of cryotreated tool steel

3.6.1 Mild Wear Regime

The mild wear regime is confined in between HTTT and 16 h of cryosoaking time, as clearly indicated in Fig. 11. The worn surface of HTTT, as depicted in Fig. 12, shows deformation marks, visible sliding marks along with carbides and wear cavities due to dislodgement of wear particles all primarily as a result of plastic deformation of surface in accordance to Suh theory [16]. During this regime, increase in hardness is noticed (Fig. 4) with corresponding increased precipitation of tertiary carbides (Fig. 3). Carbides exhibit high hardness, offer resistance to deformation during sliding of the surface and hence help the reduction in wear rate. This fact is further explored using 2D contour (Fig. 15) which reveals dominance of delamination wear mode.

3.6.2 Mild-Stable Transitions Wear

Figure 13 shows mixed-mode wear consisting partly of deformation marks indicating isolated spots of dislodgement

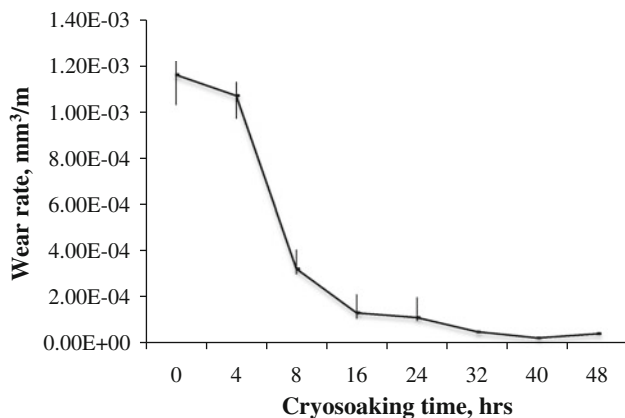


Fig. 11 Wear rate variation as a function of cryosoaking time

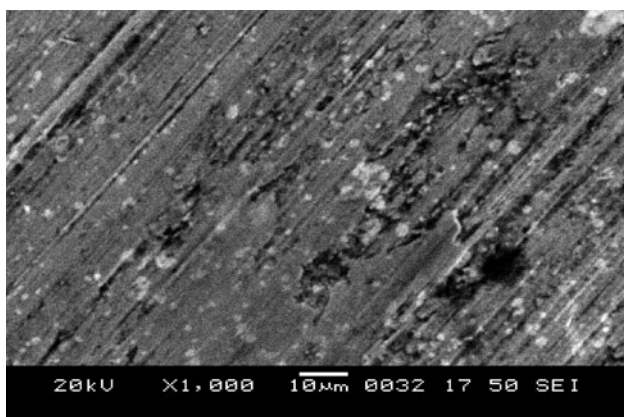


Fig. 12 Worn surface of HTTT depicts deep grooving marks/ridges along the sliding direction indicating carbides and wear cavity due particle dislodgement

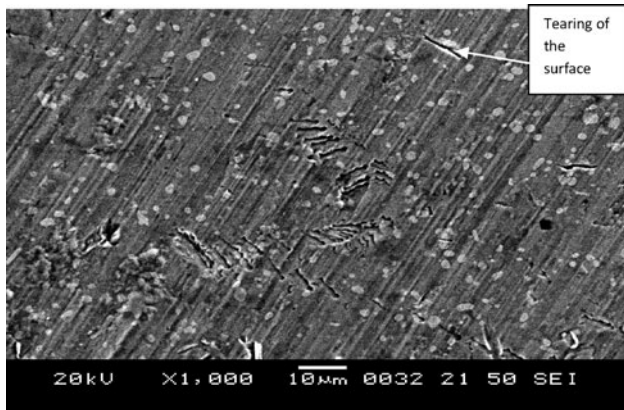


Fig. 13 Worn surface of HTC (16 h) depicts severe-mild transition wear with shallow grooving along the sliding direction with indication of carbides and cracks due to tearing of the surface

of wear particles and partly of adhesive wear mode as a result of deformation of the surface observed at 16 h of cryosoaking time. With reference to HTTT, the transition

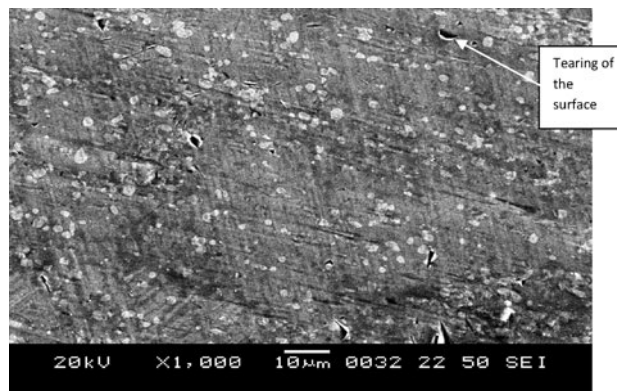


Fig. 14 Worn surface of HTC (48 h) depicts adhesive wear mode with smooth deformed layer surface with visible carbides depicting wear stabilisation

point corresponds to 90 % decrease in wear rate with concurrent increase in hardness to 63 HRC (Fig. 2), maximum density of carbides (Fig. 6), minimum residual stress (Fig. 4) and marginal change in impact toughness (Fig. 3). Worn surface reveals numerous cracks due to tearing of the surface, which are slightly inclined to sliding direction. Such tearing of the surface could be the result of strong adhesive action of the sliding surface with the counterface.

3.6.3 Stable Wear Regime

The stable wear regime (Fig. 11) is dominating from 16 to 48 h of cryosoaking time. Figure 14 shows adhesive wear mode with smooth deformed layer having isolated cavities, indicating the possibility of dislodgement of carbides due to strong adhesive nature of the sliding surface. This stable wear regime is the result of increase in hardness (Fig. 4), increase in tertiary carbide density (Fig. 3), increase in compressive residual stress (Fig. 6) and maximum impact energy (Fig. 5). With the ultrafine nature of tertiary carbides, the material offers resistance to the flow of deforming surface and thereby reduces the wear of the surface with some localized tearing spots. Figure 15 shows microstructural development beneath the wear surface indicating numerous tearing marks in the deformed subsurface. The dominance of the wear mechanism is quantified from the 2D contour (Fig. 16) which clearly delineates adhesive wear mode from delamination wear mode. It may be noted from Fig. 16b that the low wear iso-wear rate contour lines lies at higher cryosoaking time and high hardness and vice versa.

4 Conclusions

Based on the forgoing discussion on the results, the following conclusions can be drawn:

Fig. 15 SEM microstructure beneath wear surface shows subsurface deformation and dislodged cavities with tearing of the deformed subsurface depicts delamination wear

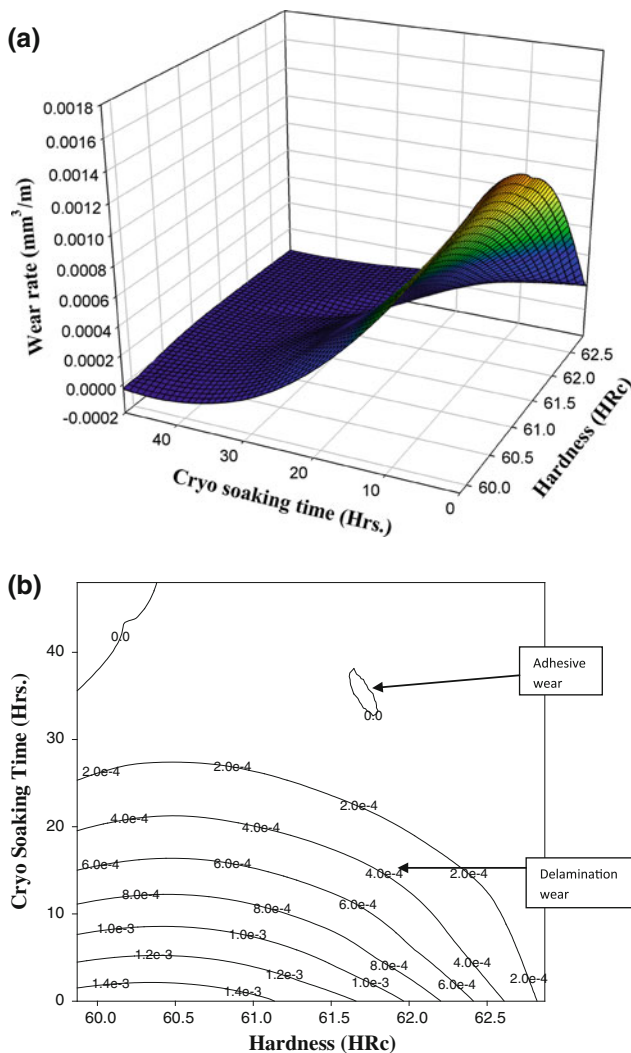
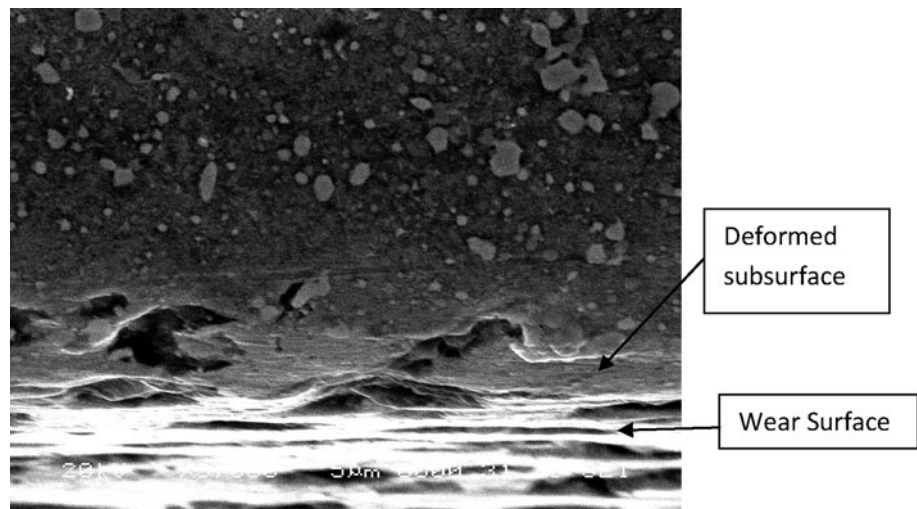


Fig. 16 Wear surface response (a) and its 2D contour depicts mild wear mode and adhesive wear mode (b)

- (a) All cryotreated specimens exhibited higher percentage of FC than CC. Nucleation and growth of carbides were the competing reactions which decide the carbide density and thus varied with cryosoaking time.
- (b) Wear complexity has been studied by plotting individually hardness, carbide density, impact toughness and compressive residual stress against wear rates. Analysis reveals contribution of these influencing factors on wear rates.
- (c) Wear rate is dramatically reduced by 90 % at HTC16 and attains steady state thereafter, called as wear stabilisation.
- (d) Wear surface response and 2D contour delineates wear mechanism in the form of mild wear regime with dominance of delamination wear mode. Whereas stable wear regime with dominance of adhesive wear mode results in lowest wear rate regime thus leading to wear stabilisation.

Acknowledgments Authors gratefully acknowledge the financial support from Department of Science and Technology (DST) for funding the project and VNIT Nagpur for extending the SEM facility, and also thank Prof. P. R. Khangoankar for his valuable inputs.

References

da Silva F J, Franco S D, Machado A R, Ezugwu E O, and Souza Jr A M, *Wear* **261** (2006) 674.
 Molinari A, Pellizzari M, Gialanella S, Straffelini G, and Stiasny K H, *J Mater Process Technol* **118** (2001) 350.
 Barron R F, *Cryogenics* **22** (1982) 409.
 Huang J Y, Zhu Y T, Liao X Z, Beyerlein I J, Bourke M A, and Mitchell T E, *Mater Sci Eng A* **399** (2003) 241.
 Yong A, Seah K, and Rahman M, *Int J Mach Tools Manuf* **46** (2006) 2051.
 Ailincai A G, and Baciuc C, *Metall J* (1990) 283.
 Meng F, Tagashira K, Azuma R, and Soma H, *ISIJ Int* **34** (1994) 205.

- Yang H-S, Wang J, Shen B-L, Liu H-H, Gao S-J, Huang S-J, *Wear* **261** (2006) 1150.
- Leskovsek V, Kalin M, and Vizintin, *Vacuum* **80** (2006) 507.
- Firouzdor V, Nejati E, and Khomamizdeh F, *J Mater Process Technol* **206** (2008) 467.
- Kelkar R, Nash P, Zhu Y, *Heat Treat Progress* **7** (2007) 55.
- Ahsan Ali K, and Ahmed Mirghani I, *J Mater Process Technol* **196** (2008) 149.
- Das D, Dutta A K, and Ray K K, *Cryogenics* **49** (2009) 176.
- Robert E, *Physical Metallurgy Principles*, 2nd edn. EWP, New Delhi (1973).
- Dhokey N B, and Nirbhavne S, *J Mater Process Technol* **209** (2009) 1484.
- Suh N, and Th Archard J F, *J Appl Phys* **24** (1953) 981.